THE JOURNAL OF PHYSICAL CHEMISTRY C

Article

pubs.acs.org/JPCC

Chemical Visualization of Asphaltenes Aggregation Processes Studied in Situ with ATR-FTIR Spectroscopic Imaging and NMR Imaging

Anton A. Gabrienko,[†,‡] Evgeny V. Morozov,[§,∥,⊥] Velu Subramani,[#] Oleg N. Martyanov,*[,‡,△] and Sergei G. Kazarian*[,†]

[†]Department of Chemical Engineering, Imperial College London, South Kensington Campus, London, United Kingdom SW7 2AZ

[‡]Boreskov Institute of Catalysis, Siberian Branch of the Russian Academy of Sciences, Prospekt Akademika Lavrentieva 5, Novosibirsk 630090, Russia

[§]Institute of Chemistry and Chemical Technology, Siberian Branch of the Russian Academy of Sciences, Akademgorodok 50/24, Krasnoyarsk 660036, Russia

[∥]Kirensky Institute of Physics, Siberian Branch of the Russian Academy of Sciences, Akademgorodok 50/38, Krasnoyarsk 660036, Russia

[⊥]UNICAT Ltd., Akademika Lavrentieva 5, Novosibirsk 630090, Russia

[#]BP Products North America, Inc. Refining and Logistics Technology, Naperville, Illinois 60563, United States

[△]Novosibirsk State University, Pirogova street 2, Novosibirsk 630090, Russia

ABSTRACT: Crude oil phase behavior and asphaltene precipitation have been studied by two complementary chemical imaging methods for the first time. ATR-FTIR spectroscopic imaging approach has revealed the chemical composition of agglomerated and precipitated asphaltenes upon dilution with a flocculant. Asphaltenes, containing oxygen and nitrogen heteroatomic functional groups, have been detected to be least stable. Aromatic abundant asphaltenes have been observed to have relatively high solubility in crude oil/heptane blends. NMR imaging approach, capable of imaging in the bulk of crude oil samples, has demonstrated that *n*-heptane causes aggregation which can lead to the stable suspension or to the sedimentation followed by the formation of deposits, depending on flocculant concentration. These processes have been monitored for small and large amounts of heptane added to crude oil. The data obtained by ATR-FTIR spectroscopic imaging and NMR imaging have been correlated to propose a possible link between the chemical structure of asphaltenes and a mechanism of the formation of deposits.

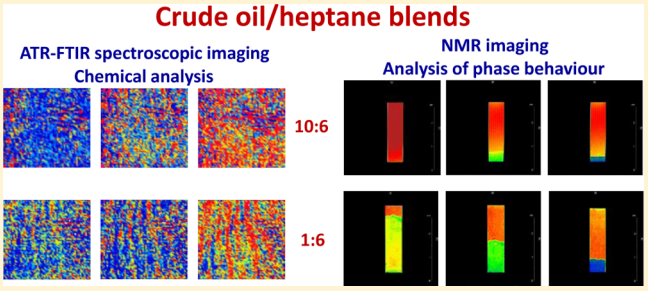

1. INTRODUCTION

Nowadays, the petroleum industry faces the challenging issue of processing heavy and opportunistic crude oils which is not only expensive but also very complex due to the necessity to refine the most abundant feedstock with the heaviest constituents, such as resins, asphaltenes, and maltenes. Understanding the crude oil properties and behavior is key for effective processing and utilization of such opportunistic crude oils. Significant progress has been made in studies of crude oils and their separate constituents in both laboratory and industrial conditions.[1] Great attention has been paid to specific asphaltene fractions to investigate their chemical structure, physical properties, and phase behavior.[2−5] Accumulated data can potentially help to predict and avoid possible problems, such as fouling and deposition, and select optimal parameters for particular operational conditions.

Based on available data presented in the literature, one can state that there are two main ways to describe the asphaltene behavior in crude oil. The first one is solution theory, which states that asphaltenes and resins are molecular entities dissolved in crude oil.[6,7] According to another proposed theory, asphaltene and resin molecules form asphaltene−asphaltene and asphaltene−resin aggregates dispersed in crude oil media.[8−10] Both of these theories include different models, interpreting various experimental observations and data.[11−13] Nevertheless, the generally accepted fact is that asphaltenes do exhibit colloidal behavior resulting in association and aggregation processes followed by precipitation under some external factors, such as temperature, pressure, and chemical composition changes.[13]

To investigate the issues related to crude oil properties, the following methods are commonly used: infrared (IR) and

Received: November 28, 2014
Revised: January 5, 2015
Published: January 7, 2015

DOI: 10.1021/jp511891f
J. Phys. Chem. C 2015, 119, 2646−2660

nuclear magnetic resonance (NMR) spectroscopy, electron spin resonance (ESR), small-angle neutron and X-ray scattering, calorimetry, dynamic light scattering, ultracentrifugation, optical and electron microscopy, etc.[14−29] The most generally accepted way to study precipitation from crude oil is titration with an antisolvent such as *n*-alkanes (typically heptane or pentane). It allows determining the onset of precipitation, the amount of material precipitated, and the solubility of asphaltenes.[11,12,30] Such information plays an important role in the understanding of precipitation mechanisms and factors that influence the asphaltenes phase behavior. To study complex phase behavior in crude oil systems subjected to *n*-alkanes properly, in situ methods, which are capable of analyzing chemical composition and carrying out experiments in a wide spatial and time scale, are required.

Fourier transform infrared (FTIR) spectroscopy has been widely used to analyze crude oil and asphaltene composition.[31−43] Recently, an attenuated total reflection Fourier transform infrared (ATR-FTIR) spectroscopic imaging approach, which can provide chemical information about heterogeneous samples on the microscale, has been developed and utilized to study heat exchanger deposits[44] and behavior of crude oils in situ.[45,46] Magnetic resonance imaging (MRI) is a well-known noninvasive and sufficiently informative technique. It was first developed for medical applications but now is actively used and integrated in chemical engineering and materials science. Sol−gel transfer, polymerization and cementation processes, sedimentation, chemical waves propagation, various catalysts materials, and heavy crude oils have been successfully studied by MRI.[47−55] The MRI method usually provides a spatial resolution no better than tens of microns and can study bulk phases on a macroscale.

The advantages and capabilities of these approaches, ATR-FTIR and NMR spectroscopic imaging, to study heterogeneous samples with relatively high spatial resolution, to carry out experiments using an in situ regime, to obtain chemical and physical information about the monitored processes give reasonable expectations to obtain new valuable data related to crude oil and asphaltene properties, particularly when both techniques are applied to the same oil samples. An exciting opportunity exists for in situ studies of the onset of processes of aggregation and precipitation of asphaltenes on micro- and macroscales to obtain data on the chemical composition of the precipitated species and, at the same time, to study the behavior of the bulk phases, formed by aggregated asphaltenes, on a macroscale. Therefore, these two complementary methods have been combined and applied in this work for the first time to investigate the asphaltene aggregation process in crude oil/heptane mixtures with different volume ratios.

2. EXPERIMENTAL SECTION

2.1. Samples and Materials Characterization. Table 1 shows the chemical composition of crude oils studied in this work. *n*-Heptane (≥99.0% purity) was purchased from VWR International Ltd. and used without further purification.

2.2. ATR-FTIR Spectroscopic Imaging. An IFS 66/S continuous-scan FTIR spectrometer (Bruker Optics) with a macrochamber extension and a focal plane array (FPA, 64 × 64 pixels) infrared detector was used for macro-ATR-FTIR spectroscopic imaging experiments.[44−46] A diamond ATR accessory (Imaging Golden Gate, Specac, UK) was used in the macrochamber extension for each measurement. A total of

Table 1. Chemical Composition of Crude Oil Samples

	crude oil sample		
composition (wt %)	1	2	3
saturates	21.0	18.8	23.2
aromatics	37.2	41.9	42.9
asphaltenes	6.7	6.0	2.2
total sulfur	4.1	2.2	2.0
API gravity	16.4	19.6	19.4

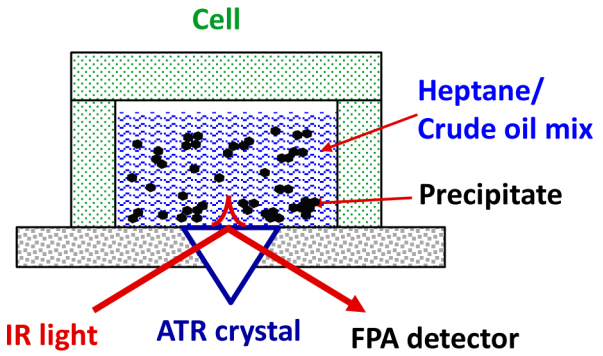

Figure 1. Schematic of the custom designed cell combined with a diamond ATR accessory for ATR-FTIR spectroscopic imaging experiments.

128 scans were accumulated for each mid-FTIR spectrum (1800−900 cm^{-1} region) with a resolution of 4 cm^{-1}.

Figure 1 shows the schematic of custom designed cell combined with an ATR accessory for in situ chemical imaging of crude oils. The bottom of the cell is the top surface of the diamond crystal which is used for ATR-FTIR spectroscopic measurements. Usually 15 μL of crude oil is placed inside the cell. After recording the crude oil spectra, a certain amount of heptane, depending on the required heptane/oil ratio, is added into the cell. Stirring is not applicable for this cell. However, the mixing of crude oil and *n*-heptane inside the cell can be easily monitored with the in situ spectroscopic imaging approach that allows detecting any inhomogeneity of the studied system. One can monitor the mixing of crude oil and heptane in situ using this spectroscopic imaging approach. For instance, the first and second rows in Figures 3−5 show the chemical images of crude oil/heptane blends recorded just after mixing and several minutes after mixing. Based on the comparison of these images, it was concluded that crude oil and heptane blends become homogeneously mixed within a few minutes after the addition of heptane to crude oil even in cases where there is relatively low heptane concentration. Taking into account the fact that the shortest time after which precipitation was observed in this work was 10 min we could conclude that a mixing process will have little or no effect on the results obtained. The result for each experiment (at particular heptane/oil ratio) was validated by three repetitions. The FTIR data presented in this study are reproducible.

It is important to note that, the strong absorption of crude oil and its deposits in the infrared region presents a challenge for measurements in transmission mode, thus the ATR-FTIR spectroscopic imaging approach provides a unique opportunity to study in situ crude oil behavior and particularly precipitation of asphaltenes. However, a few points related to the experimental procedure should be mentioned. The probing depth of ATR-FTIR spectroscopy with the diamond crystal is between

DOI: 10.1021/jp511891f
J. Phys. Chem. C 2015, 119, 2646−2660

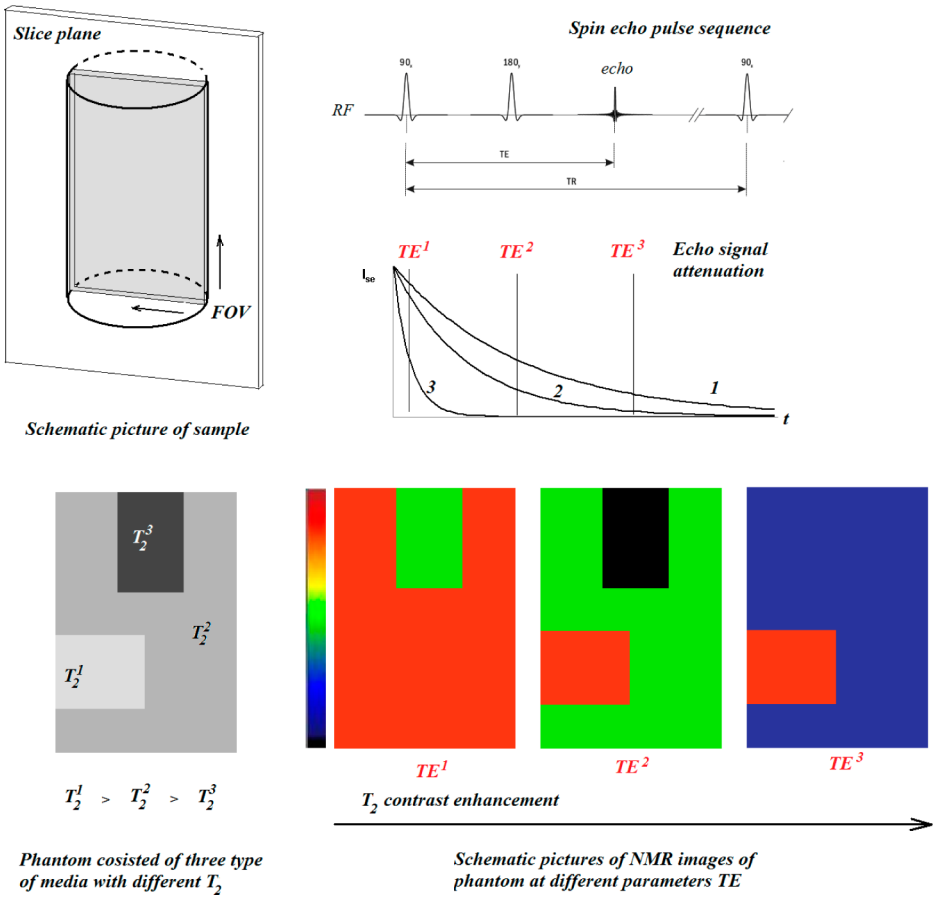

Figure 2. Schematic of the NMR imaging approach: sample slicing, adjustment of measurement parameters, and contrast enhancement of images.

1 and 5 μm, depending on the wavenumber and the refractive index of the crude oil. Due to this fact, a relatively thin layer of the sample can be analyzed in the vicinity of the measuring surface of diamond crystal. On the other hand, this approach can measure the precipitate that formed and sank from a bulk volume of the sample. In this case, however, the crude oil viscosity can likely affect the precipitate sinking process and thus on precipitation the onset point measured. Consequently, a relatively small volume of 15−30 μL of crude oil was used to minimize the possible effect of rheological properties of the studied samples.

The focal plane array (FPA) detector employed in this study is a multichannel detector with thousands of pixels (4096 pixels), which is used for ATR-FTIR spectroscopic imaging. Such a detector allows recording of up to several thousand individual mid-IR spectra simultaneously. The images obtained with this approach are created by plotting the distribution of the integrated absorbance of a selected spectral band for each pixel as a color distribution. Thus, the color scale effectively gives the concentration distribution of the particular chemical component related to the selected spectral band within the measured area of the sample. For example, a spectral band at 1650−1550 cm^{-1} is used in this work to visualize asphaltene precipitation from crude oil.[45,46] In general, this chemical imaging approach is considered to be reliable for detection of trace materials that could be present in samples under investigation.[45,56,57] The individual detector (pixel) of a multichannel FPA measures a mid-IR spectrum from a small area of the specimen (dimensions of ca. 10−15 μm with the accessory used in this study),[58] thus providing spectral or chemical information about localized individual components without the spectral contribution of other materials which are also present in the heterogeneous sample.

2.3. NMR Imaging. The imaging experiments were carried out using NMR imaging installation based on Bruker AVANCE DPX 200:89 mm diameter vertical bore, water-cooled and self-shielded Bruker gradient set with a maximum gradient strength of 292 mT/m, Bruker RF probe PH MINI 0.75, 38 mm internal diameter birdcage coil tuned and matched to ^{1}H nuclear resonance frequency of 200.13 MHz, console operated with Paravision 4.0 software.

Crude oil samples were placed inside the glass tube (7 mm diameter) at room temperature followed by careful stirring with *n*-heptane at given ratios. The overall volume of the crude oil/heptane mixture was ca. 1 mL. After blending, the tube with the sample was inserted into the MRI probe, and the process of NMR image acquisition was started immediately. The temperature of 25 ± 2 °C was maintained during the measurement.

The NMR imaging (MRI) approach allows measuring the intensity of NMR signal that comes from the selected area of the sample (the principles of MRI are well-known and described in detail in ref 59). So, in fact using MRI one can achieve either the 2D map of signal intensity distribution, that in turn strongly correlated with local relaxation times T_1, T_2, or directly the 2D map of T_1, T_2 distribution itself. The relaxation time depends on different parameters of the system such as density, chemical shift, magnetic susceptibility, speed of flow, diffusion coefficient, and many others, because these parameters can change the correlation time of fluctuating local magnetic field via different mechanisms. Consequently, the MRI

DOI: 10.1021/jp511891f
J. Phys. Chem. C 2015, 119, 2646−2660

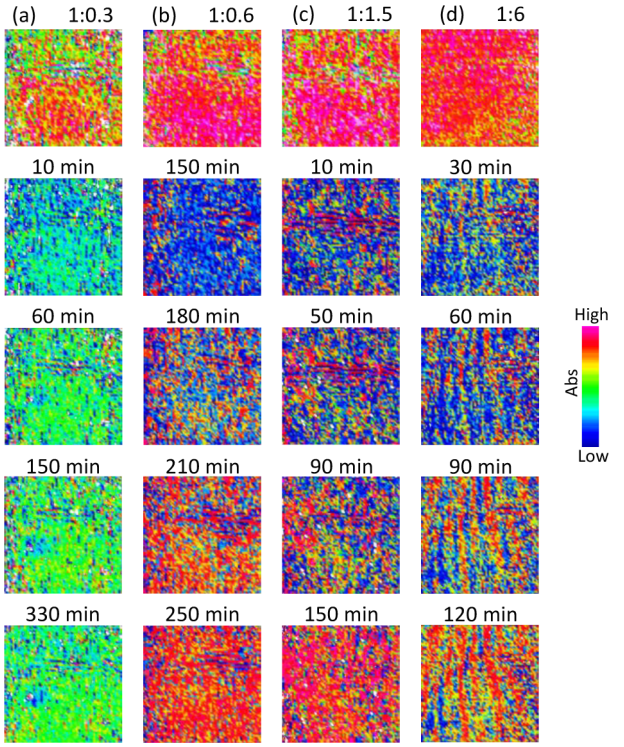

Figure 3. In situ macro-ATR-FTIR spectroscopic images of the crude oil (sample 1) and heptane system. The first row of images represents crude oil immediately after heptane addition. The columns show the dynamics of asphaltene precipitation at different crude oil/heptane volume ratios: (a) 1:0.3; (b) 1:0.6; (c) 1:1.5; and (d) 1:6, respectively. Images were obtained based on the distribution of the integrated absorbance of the spectral band at 1650−1550 cm^{-1}. The imaging area is ca. 610 μm × 530 μm.

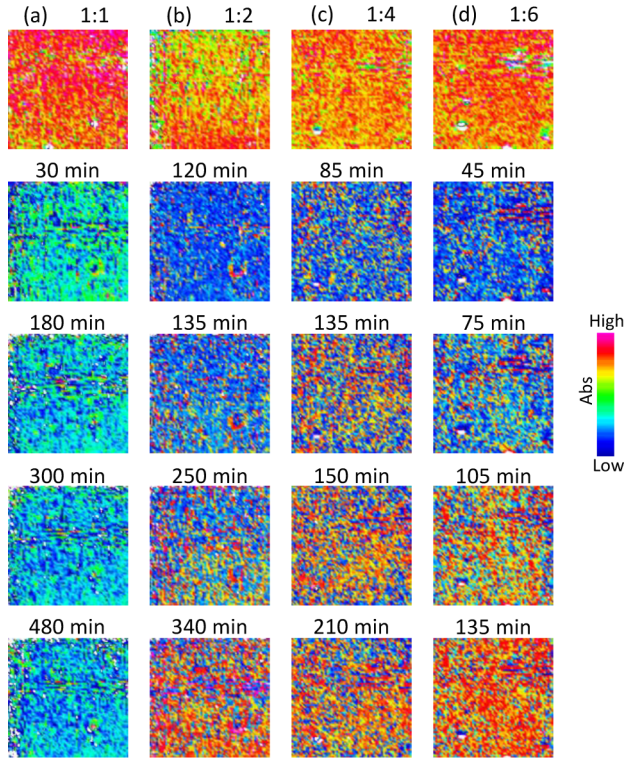

Figure 4. In situ macro-ATR-FTIR spectroscopic images of the crude oil (sample 2) and heptane system. The first row of images represents crude oil immediately after heptane addition. The columns show the dynamics of asphaltene precipitation at different crude oil/heptane volume ratios: (a) 1:1; (b) 1:2; (c) 1:4; and (d) 1:6, respectively. Images were obtained based on the distribution of the integrated absorbance of the spectral band at 1650−1550 cm^{-1}. The imaging area is ca. 610 μm × 530 μm.

method is highly sensitive to the small alteration of the system parameters and allows evaluating them simultaneously. The additional advantage of the NMR imaging approach is the opportunity to apply the technique for the optically and IR nontransparent species making it an excellent tool for the study of the bulk volume of crude oils.

To obtain an informative image, one can adjust the NMR image contrast by changing the measuring range of relaxation times T_2, where it depends mostly on the parameter that we are looking for (such type of contrast adjusting is referred to as T_2 weighting). One can do it just by changing the instrumentation parameters (time between the radiofrequency pulses, Figure 2). For the media with a short relaxation time, one needs to choose a small time scale between pulses (TE) while, for a larger relaxation time, the TE should be considerably larger to have a good contrast.

It should be mentioned that the image acquired demonstrates two or more areas (in most cases) separated by interfaces. These areas are commonly defined as "phases" in the sense of spatial domain rather than in its thermodynamic meaning, implying that all pixels inside a particular domain display similar behavior of relaxation times (or even equal T_1, T_2 itself, if the domain contains the same chemical composition or/and structure of medium within the interface). It allows a quantitative description of interface dynamics instead of the behavior of every separate pixel on the image. The description of results followed by the discussion takes into account this definition of "phase" term.

Slice selective 2D NMR images were acquired using the standard spin−echo based pulse sequence[59,60] supplied by imager software: T_2-weighted images were acquired by the Rapid Acquisition with Relaxation Enhancement (RARE) technique; T_2 maps were plotted by the processing of image sequences acquired by the Multi Slice Multi Echo (MSME) technique (using standard Image Sequence Analysis option supplied by software). The parameters of image acquisition were the following: slice thickness of 1 mm; field of view (FOV) of 40 mm; matrixes of 128 × 128, 256 × 256 and 512 × 512 pixels; time repetition (TR) and time echo (TE) were adjusted over a wide range depending on samples T_1 and T_2; the echo-train for the RARE technique consisted of 128 equally spaced echoes, the number of echoes for the MSME technique was 28. T_2 maps were used for the visualization of sharp interfaces and areas with high contrast, while T_2-weighted images, which are more sensitive (with higher resolution), were employed for the cases where diffuse interfaces or flat contrast would be expected. T_2 profiles were evaluated by plotting T_2 vs coordinate corresponding to the position of the pixel on the T_2 map (all profiles presented in this work are plotted along the vertical axis of the tube with the sample).

3. RESULTS

In this work, three crude oil samples were analyzed with ATR-FTIR and NMR imaging approaches using heptane as a titration agent to induce asphaltene precipitation. The obtained results are presented below followed by their discussion.

DOI: 10.1021/jp511891f
J. Phys. Chem. C 2015, 119, 2646−2660

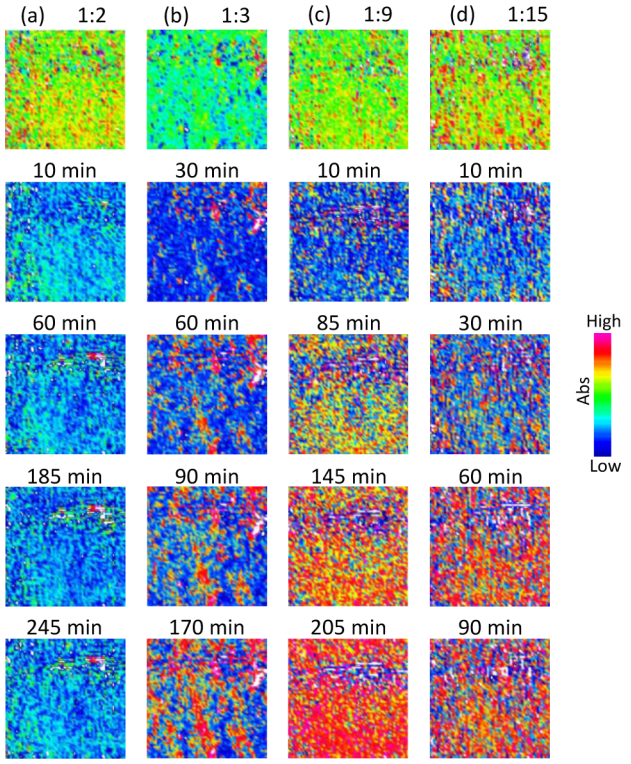

Figure 5. In situ macro-ATR-FTIR spectroscopic images of the crude oil (sample 3) and heptane system. The first row of images represents crude oil immediately after heptane addition. Columns show the dynamics of asphaltene precipitation at different crude oil/heptane volume ratios: (a) 1:2; (b) 1:3; (c) 1:9; and (d) 1:15, respectively. Images were obtained based on the distribution of the integrated absorbance of the spectral band at 1650−1550 cm^{-1}. The imaging area is ca. 610 μm × 530 μm.

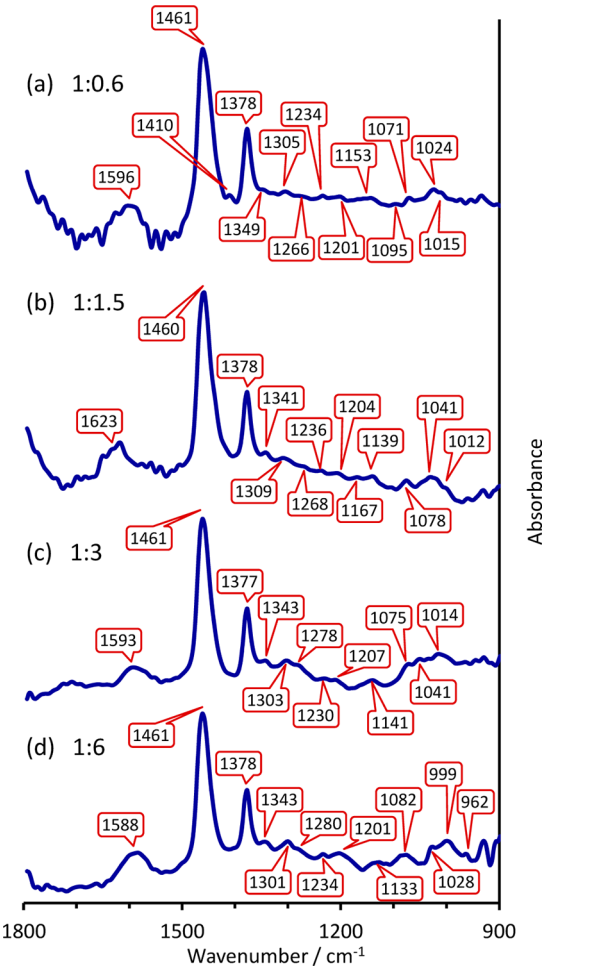

Figure 6. ATR-FTIR spectra extracted from the locations of high concentration of asphaltenes precipitated from crude oil (sample 1) at different dilution with heptane (the time passed after mixing is shown in parentheses): (a) 1:0.6 (250 min); (b) 1:1.5 (150 min); (c) 1:3 (150 min); and (d) 1:6 (120 min). The original spectra are shown, no subtraction of heptane or dissolved crude oil spectra was performed.

3.1. ATR-FTIR Spectroscopic Imaging Results. Figures 3−5 present chemical images of the studied crude oil samples. As described above, these images were created using an integrated absorbance of the band at 1650−1550 cm^{-1}, which corresponds to the stretching vibration of aromatic C═C bond. Thus, the images shown here represent the spatial distribution of aromatic hydrocarbons (simple and complex) within the measuring area of a sample using this spectral band. The first row in Figures 3−5 contains chemical images of the crude oil/heptane mixture or blend obtained immediately after heptane addition to crude oil. The main false color of the images depends on the concentration of aromatic hydrocarbons and scale chosen for better presentation. Hence, these images are mostly red, yellow, and green thus indicating relatively high concentration and homogeneous distribution of aromatic components. The columns in Figures 3−5 show the time dependence of aromatic hydrocarbons concentration in crude oil/heptane blends of a particular volume ratio. Dilution of crude oil with heptane leads to the dissolution of aromatic constituents resulting in a decrease of their concentration. In the chemical images, this process can be seen as a color change from red and yellow to green and blue where the later colors correspond to lower concentration. Usually, the crude oil dilution or dissolution process takes a few minutes and leads to a homogeneous mixture. Further, the images show no changes in color during the course of the whole experiment (few or several hours) if the amount of heptane is not sufficient to induce asphaltene precipitation (Figures 3a−5a). On the other hand, the red/yellow isolated spots followed by bigger patterns appear in the images (Figures 3b−d, 4b−d, and 5b−d) if the heptane volume added to crude oil is high enough to destabilize asphaltene molecules. These spots and patterns are shown in red and yellow, which correspond to a relatively high concentration of complex aromatic hydrocarbons, indicating the formation of precipitate particles in particular regions of the measured sample area. Further, the chemical composition of observed precipitate can be determined by selected ATR-FTIR spectra analysis. Thus, the ATR-FTIR spectroscopic imaging approach provides an opportunity to monitor in situ processes and chemically analyze the precipitation process due to its ability to spatially study heterogeneous samples.

It should be noted that in some cases (Figures 3d and 5b) a stripped pattern can be seen in the chemical images. This can be interpreted as the precipitated particles forming a structure which is caused as a result of the experimental conditions used (for instance heptane concentration). The formation of suspensions and gel-like deposits of asphaltenes was monitored with the NMR imaging approach (see section 3.2). In this case, the deposit probably has a structure that can be seen in the images obtained by ATR-FTIR spectroscopic imaging.

DOI: 10.1021/jp511891f
J. Phys. Chem. C 2015, 119, 2646−2660

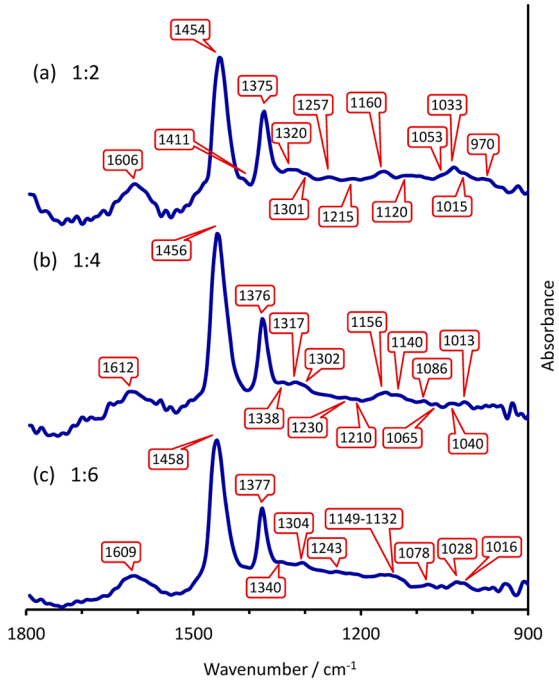

Figure 7. ATR-FTIR spectra extracted from the locations of high concentration of asphaltenes precipitated from crude oil (sample 2) at different dilution with heptane (the time passed after mixing is shown in parentheses): (a) 1:2 (340 min); (b) 1:4 (210 min); and (c) 1:6 (135 min). The original spectra are shown, no subtraction of heptane or dissolved crude oil spectra was performed.

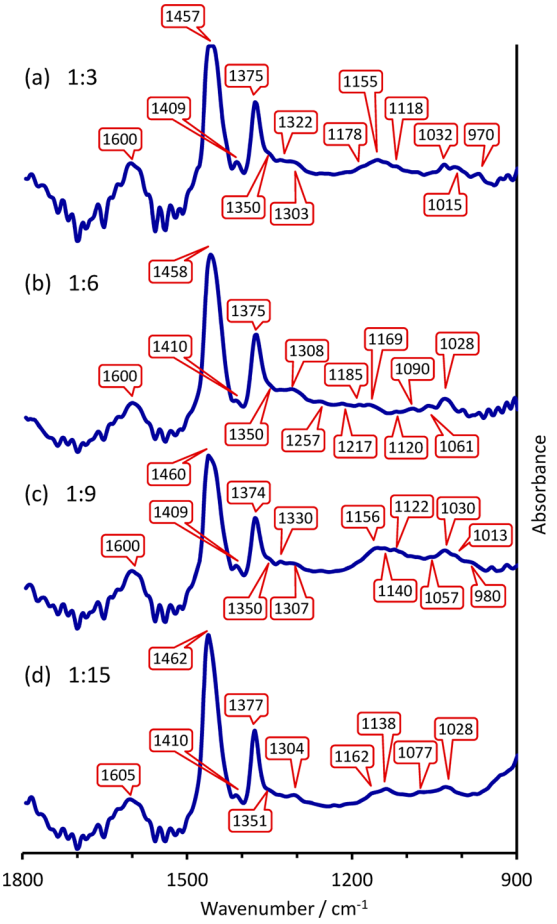

Figure 8. ATR-FTIR spectra extracted from the locations of high concentration of asphaltenes precipitated from crude oil (sample 3) at different dilution with heptane (the time passed after mixing is shown in parentheses): (a) 1:3 (170 min); (b) 1:6 (200 min); (c) 1:9 (205 min); and (d) 1:15 (90 min). The original spectra are shown, no subtraction of heptane or dissolved crude oil spectra was performed.

Selected ATR-FTIR spectra were used to perform chemical analysis of the observed precipitates (Figures 6–8). For that, the spectra were extracted from obtained imaging data sets followed by comparison with the spectra of crude oil constituents dissolved in heptane or pure heptane. The comparison was carried out both qualitatively and by spectral subtraction to validate that selected spectra do not contain spectral bands of either heptane or crude oil constituents dissolved in *n*-heptane. However, only the original selected spectra are presented in Figures 6–8. This procedure allows the assignment of the spectral bands which belong to the precipitated species only. The spectra of crude oil constituents dissolved in heptane can also be extracted from the imaging data sets. For example, Figure 5b (second row) presents the image of sample 3 at 30 min after heptane addition. The precipitate formed is indicated by the red and yellow spots, while blue shows crude oil components dissolved in heptane. Thus, by extracting spectra from differently colored areas of this image, one can obtain spectra for precipitate and crude oil fractions dissolved in *n*-heptane.

The analysis of the spectra for samples 1, 2, and 3 at different crude oil/heptane ratios gives the following. In each case, the precipitation of asphaltenes was detected. The spectral bands at 1623–1588, 1307–1303, 1138–1133, 1028, 1016, and 980–970 cm^{-1} were observed in all spectra of precipitates (Figures 6–8). These bands are typical for polycyclic aromatic hydrocarbons[61] which are the main component of asphaltene molecules. Further analysis reveals that chemical components of asphaltenes precipitated (apart from polycyclic aromatic hydrocarbons) vary depending on heptane amount added to crude oil.

Thus, the presence of the oxygen-containing species was observed as major heteroatomic constituents in asphaltene molecules precipitated at ratios 1:0.6, 1:2, and 1:3 (and 1:6) for samples 1, 2, and 3, respectively (Figures 6a, 7a, and 8a,b). Indeed, the following bands are in the spectra: 1411–1409, 1350–1349, 1033–1032, 1024, 1015 cm^{-1} are due to sulfoxide −SO− groups and 1325–1320, 1140–1130 cm^{-1} are due to sulfone $-SO_2-$ groups;[62] 1266–1257, 1244 cm^{-1} are due to aromatic ethers Ar−O−R and 1217–1215, 1185–1153, 1120–1118, 1095–1090, and 1053–1052 cm^{-1} are due to C−O bond stretching of ethers or esters.[41]

The precipitation of asphaltenes containing mostly nitrogen heteroatoms has occurred when samples 1, 2, and 3 are diluted with heptane at ratios of 1:1.5 (and 1:3), 1:4, and 1:9, respectively. This conclusion is based on the corresponding spectral analysis (Figures 6b,c, 7b, and 8c) which results in the detection of the bands at 1330–1317, 1236–1230, 1210–1204, 1140, 1086–1075, 1057–1040, and 1014–1012 cm^{-1}. This indicates that nitrogen atoms are introduced in asphaltenes in the form of pyrrole and pyridine groups.[63]

The chemical composition of asphaltene molecules that precipitate at crude oil/heptane ratios of 1:6, 1:6, and 1:15 for samples 1, 2, and 3, respectively, was also studied using the selected ATR-FTIR spectra (Figures 6d, 7c, and 8d). Thus, these asphaltenes are mostly presented by polycyclic aromatic hydrocarbons that are supported by the observation of corresponding spectral bands (see the list of these bands above).

DOI: 10.1021/jp511891f
J. Phys. Chem. C 2015, 119, 2646–2660

Table 2. Spectral Bands Observed in Selected ATR-FTIR Spectra of the Species Precipitated from Crude Oils

figure	spectrum	spectral bands/cm^{-1}	assignment
6	a	1596, 1305, 1138	polycyclic aromatics
		1410, 1349, 1024; 1325, 1130	sulfoxides; sulfones
		1266	aromatic ethers
		1201, 1153, 1095, 1071	ethers and esters
	b	1623, 1309, 1139	polycyclic aromatics
		1268, 1236, 1204	ethers and esters
		1330, 1236, 1204, 1139, 1078, 1041, 1012	pyrroles, pyridines
	c	1593, 1303, 1138	polycyclic aromatics
		1278, 1230, 1207	ethers and esters
		1327, 1230,1207, 1140, 1075, 1041, 1014	pyrroles, pyridines
	d	1588, 1301, 1133, 999, 962	polycyclic aromatics
		1343, 1234, 1082, 1028	thiophenes
7	a	1606, 1301, 1138, 970	polycyclic aromatics
		1411, 1350, 1033, 1015; 1320, 1130	sulfoxides; sulfones
		1257	aromatic ethers
		1215, 1160, 1120, 1053	ethers and esters
	b	1612, 1302, 1140	polycyclic aromatics
		1156, 1065	ethers and esters
		1317, 1230, 1210, 1140, 1086, 1040, 1013	pyrroles, pyridines
	c	1609, 1304, 1149−1132, 1016	polycyclic aromatics
		1340, 1243, 1078, 1028	thiophenes
8	a	1600, 1303, 1138, 970	polycyclic aromatics
		1409, 1350, 1032, 1015; 1322, 1130	sulfoxides; sulfones
		1178, 1155, 1118	ethers and esters
	b	1600, 1308, 1133	polycyclic aromatics
		1410, 1350, 1028	sulfoxides
		1257	aromatic ethers
		1217, 1185, 1169, 1120, 1090, 1061	ethers and esters
	c	1600, 1307, 1140, 980	polycyclic aromatics
		1409, 1350	sulfoxides
		1156, 1122	ethers and esters
		1330, 1230, 1204, 1140, 1057, 1030, 1013	pyrroles, pyridines
	d	1605, 1304, 1138, 1028	polycyclic aromatics
		1410, 1351, 1028	sulfoxides
		1161	ethers

However, there are some minor chemical differences between the samples. For example, the presence of thiophene (1343−1340, 1243−1234, 1080−1078, 1028 cm^{-1})[63] was detected in the case of samples 1 and 2 (Figures 6d and 7c). For sample 3 (Figure 8d), the asphaltenes precipitated contain sulfoxide (1410, 1351, 1028 cm^{-1}) and C−O (1162 cm^{-1}) groups.

Dilution of crude oil samples with larger amounts of heptane leads to the precipitation of asphaltenes which are similar in chemical composition to that described for ratios of 1:6, 1:6, and 1:15 for samples 1, 2, and 3, respectively. So, the precipitation of mostly polycyclic aromatic asphaltenes was detected under a relatively high concentration of heptane.

Table 2 summarizes the wavenumbers described above and their assignments to certain functional groups or chemicals.

Three points should be noted for understanding of the presented spectra. First, spectral bands corresponding to different chemical components or functional groups of asphaltenes sometimes have similar or a very close position in a spectrum. This means that such bands are identified as having the same wavenumbers due to band overlap. Second, the bands having fairly similar wavenumbers were assigned to the same chemical species observed in separate spectra. This can be explained by various possible structures of asphaltene molecules or the degree of asphaltene aggregation and interaction thus resulting in different wavenumbers. Third, presented and described spectra do not contain exclusively the bands that were mentioned in each particular case. For instance, the spectrum in Figure 8c contains not only the spectral bands of pyrrole and pyridine species, but also the bands which can be assigned to sulfoxide or C−O functional groups. Similar examples can be shown using other spectra of precipitated

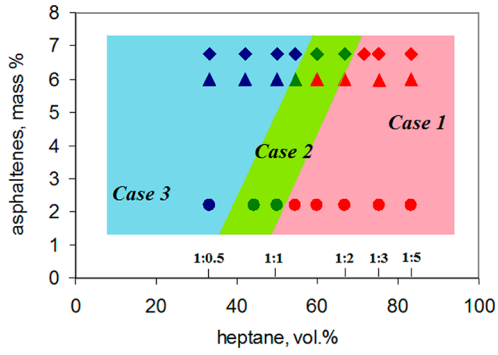

Figure 9. Diagram of the main types of crude oil/heptane behavior. Crude oil sample 1 is presented by diamonds, sample 2 by triangles, and sample 3 by circles. Heptane vol % and crude oil:heptane volume ratios are depicted along the *X*-axis.

DOI: 10.1021/jp511891f
J. Phys. Chem. C 2015, 119, 2646−2660

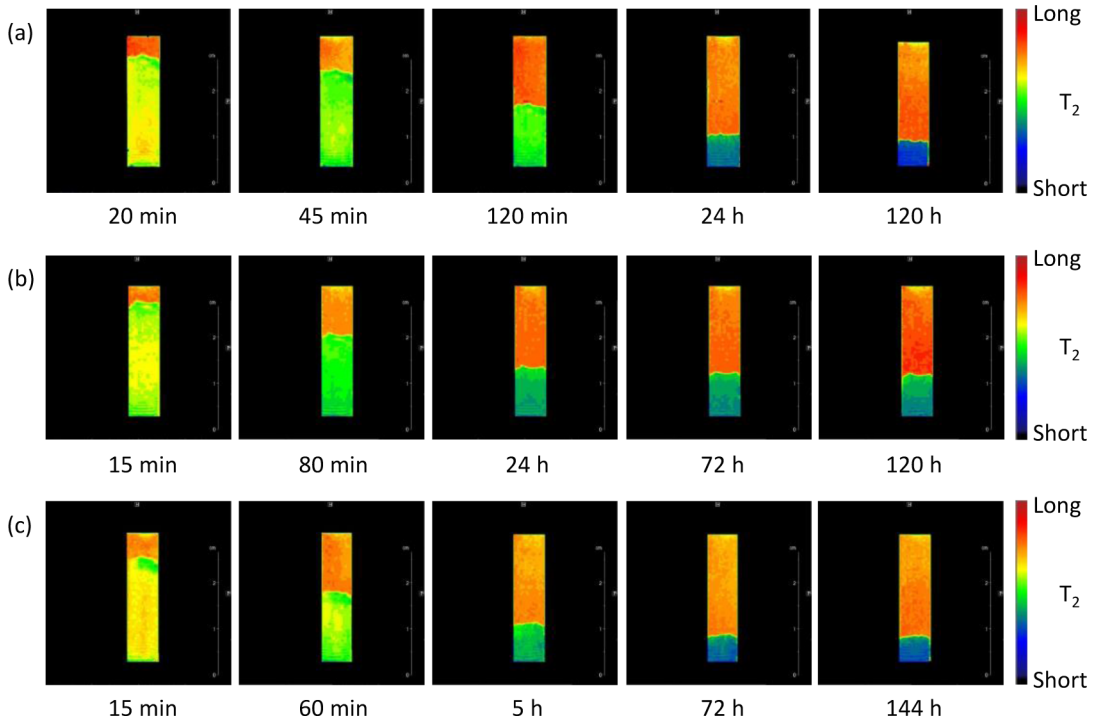

Figure 10. T_2 maps of vertical central slices in the course of crude oil/heptane system (volume ratio 1:5) evolution: sample 1 (a), 2 (b), and 3 (c). The domain consisting of an oil/heptane blend is represented by red (orange) whereas asphaltenes-enhanced suspension is represented by yellow and green, slowly transient into blue during the compaction and formation of deposit.

asphaltenes. So, this means that we do not observe the separate precipitation of chemically individual asphaltenes induced by different amounts of heptane, but normally the mixture of various asphaltenes with the prevalence of some particular components or functional groups has been observed. These prevalent components were the species that are listed and described above for each crude oil sample and crude oil/heptane dilution ratio.

3.2. NMR Imaging Results. The precipitation of asphaltenes is a consequence of the aggregation process that occurs in the bulk of the crude oil. Since ATR-FTIR spectroscopic imaging approach tests a relatively thin layer (1−5 μm) near the bottom of the sample, as was mentioned above, the behavior of bulk phases formed by aggregated asphaltenes can be studied by NMR imaging. Based on the results obtained with the MRI method for the different oils and the wide range of oil/heptane ratios, three main types of crude oil behavior can be observed: the fast aggregation process in the bulk followed by the formation of suspension with further shaping and packing of the deposits (Case 1, red area in Figure 9), rather slow formation of the sediment-like deposits near the bottom of the sample without noticeable (within MRI resolution) aggregation in the bulk of the crude oil (Case 2, green area), and no considerable deposit formation (Case 3, blue area). According to the MRI data, the structure and properties of deposits within the areas depicted in Figure 9 are quiet similar for different crude oil samples, which allows us to describe the results obtained for every case following this *three-type* classification.

Case 1: Substantial Excess of Flocculant. NMR images (Figure 10) clearly demonstrate the appearance of two bulk phases (stratification), having remarkably different spin−spin relaxation times (T_2), in crude oil/heptane systems almost immediately after components blending. The upper phase is characterized by a relatively long T_2 relaxation time with the uniform distribution within the phase area. Hence, this phase is homogeneous and consists of crude oil components dissolved in heptane. Conversely, the lower phase, possessing shorter T_2 relaxation time with slightly nonuniform initial distribution, is inhomogeneous and should be considered as those comprising the aggregates of asphaltenes that form suspension. The T_2 relaxation time distributions over the samples during evolution are presented on profiles in Figure 11. In the course of evolution (time), the interface of two separate phases moves downward in a nonlinear manner with the simultaneous decrease of mean T_2 relaxation time of the lower phase. At the same time, the upper phase keeps the initial T_2 relaxation time that is clearly demonstrated by Figure 11. Such changes of T_2 relaxation time for the lower phase indicate the compaction of suspension as the increase of mean density, which was followed by formation of the deposit phase.

Case 2: Medium Concentration of Flocculant. Decrease in the flocculant concentration in the crude oil/heptane system leads to another type of behavior. The NMR images (Figure 12) demonstrate slow formation of a new phase with a diffuse interface near the bottom of a sample. It is observed by tracking the T_2 relaxation time within the sample and detecting T_2 changes in the near bottom region, where spin−spin relaxation time becomes shorter compared with other parts of the system. Both upper and lower parts are considered to be homogeneous with the former having longer T_2 relaxation time. Contrary to Case 1, the formation of the interface in the top part of the samples was not observed. Additionally, the thickness of the deposit in the near bottom region first increases (interface moves upward), but further evolution results in a thickness decrease. During this process, the T_2 relaxation time uniformly reduces within the bulk of the deposit (T_2-profiles are presented in Figure 13). T_2 relaxation time for the upper

DOI: 10.1021/jp511891f
J. Phys. Chem. C 2015, 119, 2646−2660

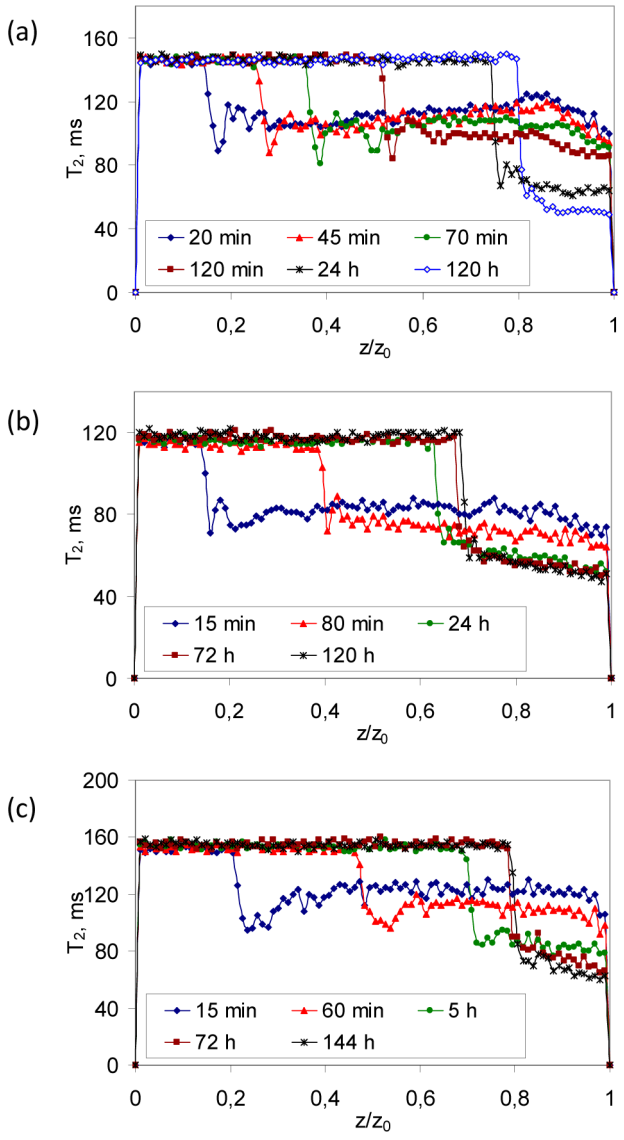

Figure 11. T_2 profiles for the crude oil/heptane system evolution (volume ratio 1:5): sample 1 (a), 2 (b), and 3 (c).

part shifts to slightly higher values indicating changes of composition or/and structure of the crude oil within this part.

Case 3: Low Concentration of Flocculant. The crude oil/heptane systems with very low flocculant concentration do not show any phase separation (Figure 14). The corresponding T_2 profiles confirm constant and uniform distribution of relaxation times over the sample during the week-long period of experiment.

It is important to note that the areas depicted in Figure 9 do not have certain concentration boundaries. There is a smooth transition from one type of behavior to another. For instance, when passing from Case 1 to Case 2 (sample 1), the deposit becomes considerably inhomogeneous and its compaction is accompanied by accumulation of a small amount of precipitating particles, which form a sediment layer on the bottom within the phase of colloidal suspension (Figure 15a). When passing from Case 2 to Case 3 (for the same sample), the low concentration of heptane used is able to cause the aggregation and precipitation of only the most unstable asphaltenes. The deposit phase can be observed not earlier than 24 h after blending (the layer at the bottom part of images in Figure 15b). It is consistent with data obtained by optical microscope experiments: the time required to detect asphaltene instability, under particular conditions, can vary from hours to several weeks and even months.[64,65]

4. DISCUSSION

4.1. Complementarity of NMR Imaging and ATR-FTIR Spectroscopic Imaging Methods. First, the difference in crude oil behavior observed with ATR-FTIR spectroscopic and NMR imaging approaches should be mentioned and explained. Apparently, the minimum amount of heptane, at which asphaltene aggregation and precipitation are detected, varies for the same crude oil sample depending on the method used. Thus, the onset of asphaltene precipitation was observed with ATR-FTIR spectroscopic imaging at a crude oil/heptane ratio of 1:0.6 for sample 1 (Figure 3b), 1:2 for sample 2 (Figure 4b), and 1:3 for sample 3 (Figure 5b). On the contrary, the MRI method revealed (Figures 9 and 12) asphaltene precipitation at different crude oil/heptane ratios: sample 1, 1:1.5; sample 2, 1:1.2; and sample 3, 1:1.

Such apparent dissimilarity of the obtained results can be explained by differences in the two experimental methods and conditions used for both approaches. For ATR-FTIR spectroscopic imaging, the volume of the blends was relatively small (20−240 μL, depending on the ratio studied), and the homogeneity of self-mixing samples was verified and controlled by the method. The volume used for the MRI experiments was larger, ca. 1 mL, therefore stirring was applied to blend the crude oil and heptane properly prior to measurement. So, we do believe that the effect of blending or stirring factors is negligible.

However, the MRI approach studies the bulk of the sample, while ATR-FTIR spectroscopic imaging probes only a thin layer (few micrometers) in the vicinity of the measured surface of the ATR crystal, so at the bottom of a miniature container of crude oil, as it follows from the experimental procedures described above. Therefore, it is expected that crude oil or precipitate properties, such as viscosity, rheology, size of agglomerates, density, etc., can influence the ability of spectroscopic methods to detect precipitation at the bottom of the container.

Any precipitate formed should sink to the bottom of the container, which is the measuring surface of the ATR crystal, to be observed by the ATR-FTIR chemical imaging approach. Moreover, the precipitate particles must settle to the particular area (610 μm × 530 μm) of the ATR crystal at which the IR light is focused (which is about 10% of the surface of the bottom area of the container). Most importantly, the precipitate could float in the crude oil/heptane mixture volume without sinking or the amount of precipitate could be insufficient, and, in this case, ATR-FTIR spectroscopy will not observe precipitate. Apparently, in the case of appropriate conditions, namely high dilution of crude oil with heptane, the most unstable asphaltenes will aggregate and sink to the ATR crystal surface first, and thus these species will be detected with ATR-FTIR spectroscopy. Other more stable asphaltenes will aggregate further and will be observed by chemical imaging. However, due to relatively high concentrations, asphaltenes having different stability can aggregate and precipitate simultaneously. In this case, ATR-FTIR spectroscopy observes a few types of the asphaltenes precipitated. Nevertheless, the chemical composition of different asphaltenes can be studied by varying the heptane amount added to crude oil.

DOI: 10.1021/jp511891f
J. Phys. Chem. C 2015, 119, 2646−2660

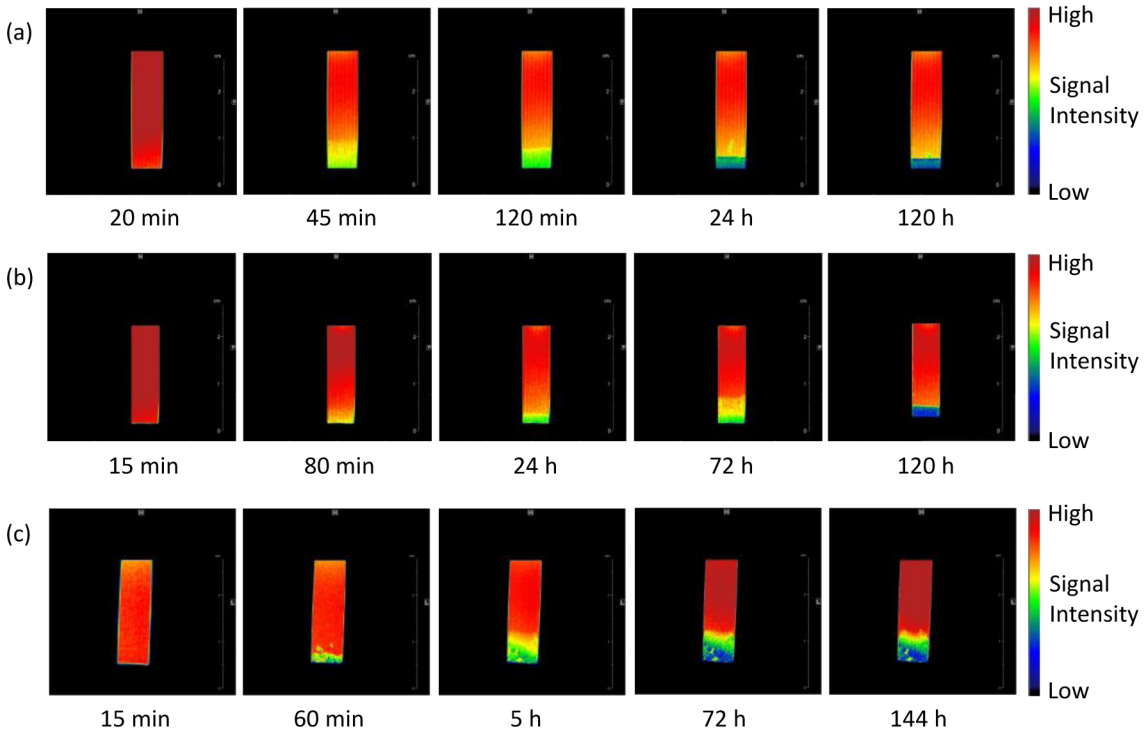

Figure 12. T_2-weighted images of vertical central slices in the course of crude oil/heptane system evolution: (a) sample 1 (ratio 1:2), (b) sample 2 (ratio 1:1.2), and (c) sample 3 (ratio 1:1). The domain consisting of an oil/heptane blend (top part of the system) is represented by red; slow accumulation of settling particles consisting of asphaltene agglomerates is represented by yellow and green. The evolution of sediment resulting in deposit formation is accompanied by a change of green into blue.

On the other hand, the MRI method has lower spatial resolution of ca. 50−100 μm compared to ATR-FTIR chemical imaging (10−15 μm), therefore the size of aggregated particles has to be large enough to be detected (basically a separate phase of precipitate should be formed). Based on this, the explanation why ATR-FTIR spectroscopic imaging detects aggregation processes for sample 1 starting from a crude oil/heptane ratio of 1:0.6, while MRI observes precipitation only at a ratio of 1:1.5, is now clear. This may mean that the asphaltene aggregation process occurs at a ratio of 1:0.6, but without precipitation, i.e. the formation of the bulk deposit phase.

Obviously, each spectroscopic approach has its own limitations and advantages. MRI probes macroscale precipitation occurring in the bulk of the sample, while ATR-FTIR spectroscopic imaging can obtain chemical information about the same sample on a microscale. The nature of ATR-FTIR spectroscopy to measure thin layers of the sample may be advantageous when the onset of precipitation, related to onset fouling, is studied. So, these two methods are complementary, and it is essential and beneficial to apply them together to get more reliable data about crude oil behavior.

4.2. Correlation between Asphaltene Chemical Composition and Precipitation Behavior. ATR-FTIR spectroscopy revealed that the chemical composition of aggregated and precipitated asphaltenes depends on the amount of heptane added to crude oil. This can be interpreted such that certain heptane volumes or concentrations cause destabilization of different asphaltenes, and thus the stability of asphaltenes depends on their chemical composition. So, it is reasonable to suppose that a small portion of heptane induces the precipitation of less stable asphaltenes, while a high heptane concentration results in the destabilization of relatively soluble species. Thus, the results obtained with the ATR-FTIR spectroscopic imaging approach allow us to correlate asphaltenes stability with their particular chemical composition. Furthermore, based on the obtained results, we propose a possible connection between the main functional groups or chemical species that asphaltene molecules contain and the tendency of asphaltenes to aggregate and precipitate following a certain behavior, which were monitored by the MRI approach in the bulk crude oil state.

As mentioned above, asphaltene molecules containing mostly oxygen heteroatoms, incorporated in the forms of sulfoxides, sulfones, ethers, and esters, aggregate and precipitate at a low concentration of heptane. Indeed, the ATR-FTIR spectra corresponding to the precipitates observed at crude oil/heptane ratios of 1:0.6 (sample 1, Figure 6a), 1:2 (sample 2, Figure 7a), and 1:3 and 1:6 (sample 3, Figure 8a,b) show spectral bands that belong to the mentioned type of functional groups. So, such oxygen-containing asphaltenes can be considered as less stable species as only a relatively small amount of heptane can be used to cause their precipitation. Asphaltene molecules incorporated by pyrrole and pyridine groups can be assigned to species with medium stability. This is due to the fact that asphaltenes having nitrogen heteroatoms in the structure were detected to be the main constituent of precipitates at intermediate crude oil/heptane ratios, namely, 1:1.5 and 1:3 for sample 1 (Figure 6b,c), 1:4 for sample 2 (Figure 7b), and 1:9 for sample 3 (Figure 8c). Dilution of crude oil with large portions of heptane results in precipitation of aromatic-abundant asphaltenes. The ATR-FTIR spectra of species precipitated at crude oil/heptane ratios of 1:6 (sample 1, Figure 6d), 1:6 (sample 2, Figure 7c), and 1:15 (sample 3, Figure 8d) show predominantly bands from complex or condensed aromatic compounds. Thus, asphaltene molecules

DOI: 10.1021/jp511891f
J. Phys. Chem. C 2015, 119, 2646−2660

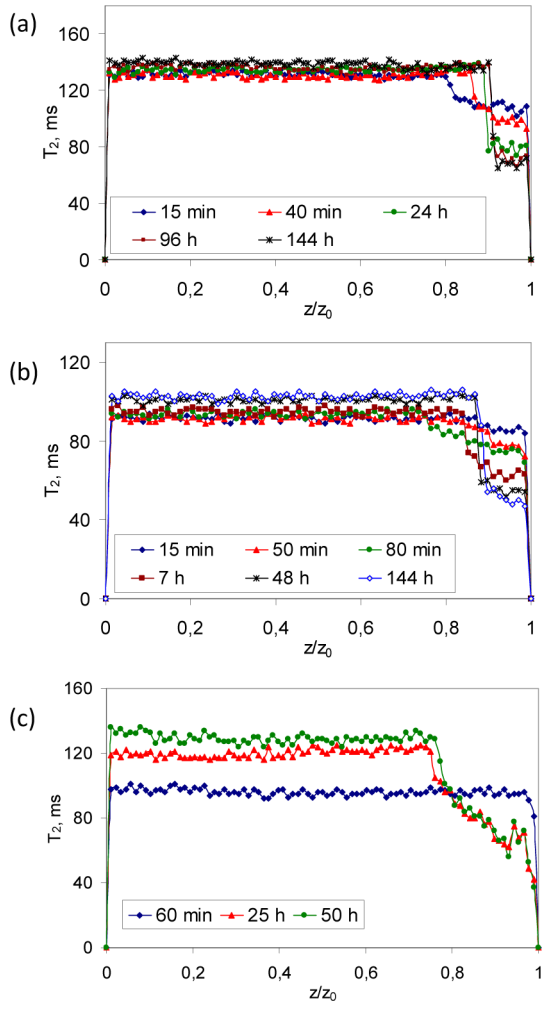

Figure 13. T_2 profiles for crude oil/heptane system evolution: (a) sample 1 (ratio 1:2), (b) sample 2 (ratio 1:1.2), and (c) sample 3 (ratio 1:1).

consisting of polycyclic aromatic hydrocarbons with the minor presence of heteroatoms seem to have relatively high stability compared to species enriched with oxygen, nitrogen, and sulfur.

Previously Hoepfner et al.[66] have studied asphaltene behavior in crude oil. The changes in fractal dimension of asphaltene clusters were observed after a small amount of heptane addition to crude oil. The largest clusters are formed by the most unstable asphaltenes which experience the strongest interaggregate attractions or weakest repulsion. Such asphaltenes are supposed to associate preferentially with one another due to strong intermolecular interactions. The interaction between asphaltene molecules that leads to their aggregation followed by precipitation is mainly associated with polycyclic aromatic sites.[67−69] However, heteroatoms present in the asphaltene molecules can give rise to dipole−dipole interaction or H-bond formation due to additional charge separation.[69−71] So, it is reasonable to suppose that asphaltenes with a particular chemical composition can have different tendencies to aggregate and thus precipitate due to various available ways of stronger intermolecular interaction.

So, taking into account our current findings, it can be proposed that asphaltenes containing oxygen and nitrogen heteroatoms (oxygen-containing asphaltenes are the least stable) have a tendency to precipitate at low heptane concentrations due to their ability for strong intermolecular interactions. Indeed, this proposition is supported by recent modeling results.[69] It was concluded that the interaction between asphaltene aromatic cores is a driving force for the association and thus aggregation. The strength of this intermolecular interaction depends on the presence of heteroatoms which can reduce the electrostatic repulsion. H-bonding was also proposed to have an effect on aggregation by providing additional association sites in large asphaltene aggregates. This is in good agreement with our results as oxygen- and nitrogen-containing functional groups can have various available ways for stronger intermolecular interactions such as dipole−dipole interactions, H-bond formation, etc. So, such asphaltenes are less stable due to a more pronounced tendency to associate and aggregate.

Similarly to the ATR-FTIR spectroscopic microscale study at the bottom of the crude oil container, the behavior of the crude oil/heptane blends was monitored with NMR imaging on the macroscale in the bulk state. The analysis of processes that occurred in the crude oil/heptane blends revealed the formation of new phases in the initially homogeneous systems for particular volume ratios. It was observed that the structure of these phases, mechanisms of their formation, and evolution strongly depend on the flocculant concentration.

For Case 1, no gradient, but uniform decrease of the T_2 relaxation time was observed for the whole deposit phase during its evolution, and the process of accumulation of the settling particles is slowed down. Hence, the deposit has a structure, which is different from that of any suspension with free gravity-driven sedimentation. The appearance of different types of sedimentation and their characterization by means of MRI have been previously described.[72] Obviously, the phase consisting of particles settling separately must form the sediment layer on the bottom of a sample with a thickness increasing over time. However, not one of the systems studied under the conditions of Case 1 demonstrates such behavior.

Based on the current MRI results in combination with those obtained by ATR-FTIR spectroscopy, the following model can be proposed. Under the acting of substantial excess of flocculant, various types of asphaltenes presented in micellar form lose their aggregation stability, including species containing the most stable functional groups (aromatic core, thiophenes). The fast aggregation processes observed by the MRI approach followed by precipitation of initial colloidal particles results in formation of a colloidal suspension consisting of agglomerates. The big size or/and branched structure of agglomerates (fractal nature of agglomerates suggested in ref 73) interacting with each other leads to the hindered particles settling[73−75] to the bottom. Thus, the hindered settling and interaction of agglomerates with each other are the reasons for transformation of the suspension into the gel-like deposit observed avoiding the accumulation of the sediment-like deposit (Figure 16).

The constant value of T_2 relaxation time for the upper phase during the whole process of system evolution (Figure 11) can be explained by the constant chemical composition: all destabilized asphaltenes have already precipitated from the solution. This proposed model is in good agreement with the data obtained by dynamic light scattering: gelation processes are suggested to be a reason for power-law collapse in the sedimentation front due to continuous aggregation of particles settling all together (reaction limited aggregation).[76−78]

DOI: 10.1021/jp511891f
J. Phys. Chem. C 2015, 119, 2646−2660

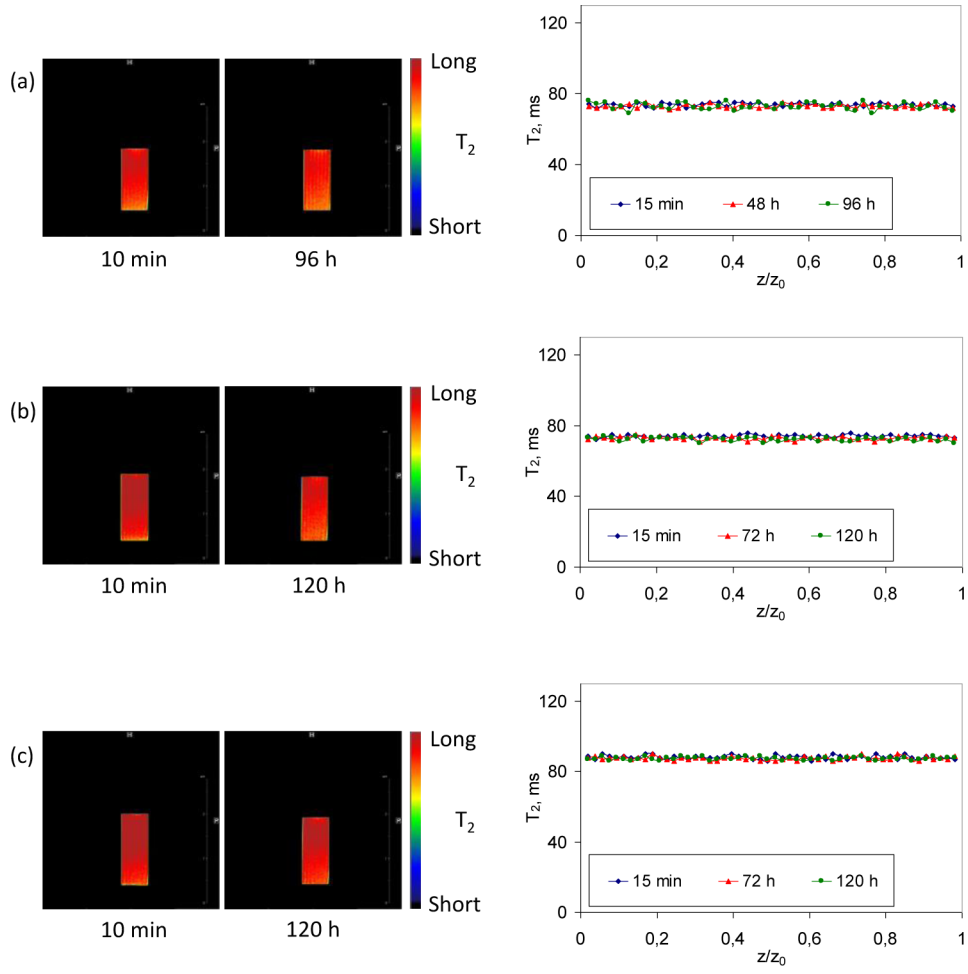

Figure 14. T_2-weighted images of vertical central slices in the course of the crude oil/heptane system (volume ratio 1:0.5) evolution with corresponding T_2 profiles: (a) sample 1, (b) sample 2, and (c) sample 3. The same color (red) on both images and the same T_2 on profiles during experiment evidently demonstrate the stability of the system composition.

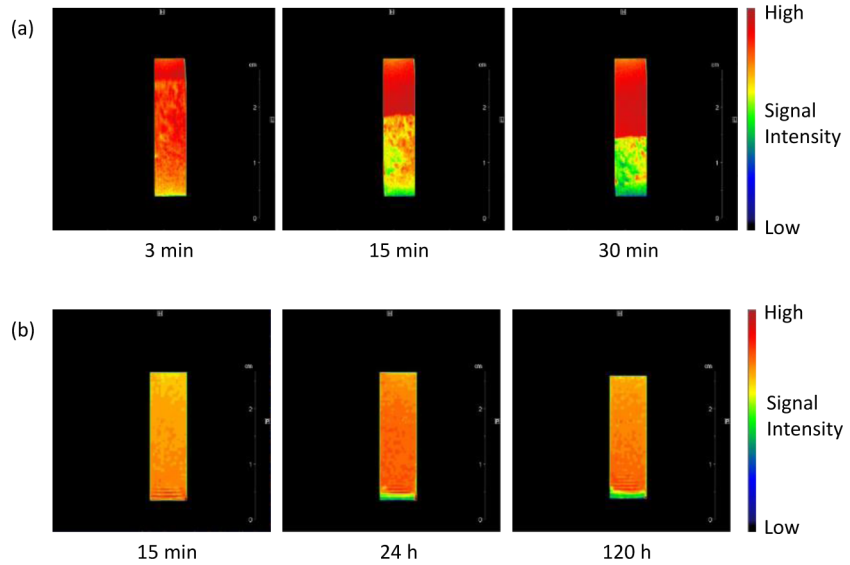

Figure 15. T_2-weighted images of the sample 1/heptane system at volume ratios of 1:2.5 (a) and 1:1.5 (b). Red (orange) represents the oil/heptane blend (top part of the systems) while suspension and deposits are represented by yellow and green.

In terms of the proposed precipitation model, Case 2 behavior of crude oil/heptane blend can be described by the following. Relatively low flocculant concentration leads to the crude oil/heptane behavior, when only certain types of asphaltenes lose their aggregation stability (the least stable having oxygen- and nitrogen-containing functional groups as

DOI: 10.1021/jp511891f
J. Phys. Chem. C 2015, 119, 2646−2660

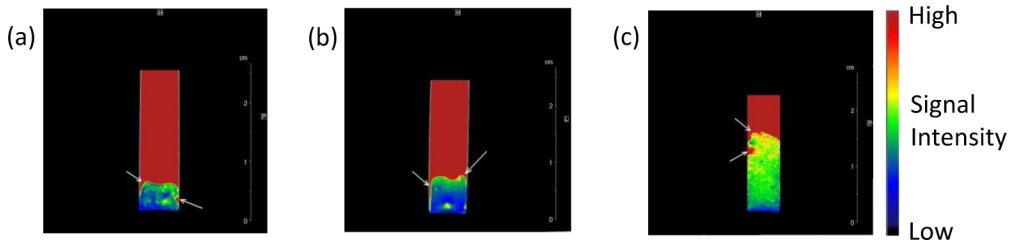

Figure 16. T_2-weighted images of deposits formed in crude oil/heptane systems: (a) sample 1 (ratio 1:2.5, 48 h after mixing), (b) sample 2 (ratio 1:2, 2 weeks after mixing), and (c) sample 3 (ratio 1:1.2, 12 h after mixing). Red represents the oil/heptane blend while deposits are represented by green and blue, depending on time of evolution.

was detected by ATR-FTIR spectroscopy). This proposition is in good accordance with recent studies, which demonstrate that upon flocculant addition to crude oil only a fraction of asphaltene nanoparticles aggregates, while the rest of the species, referred to as stable asphaltenes, remain in solution.[66] In this case, small amounts of asphaltenes, which have a tendency for strong intermolecular interactions, participate in the aggregation processes followed by settling of the slowly formed agglomerates, while another asphaltene fraction exists in a micellar form. Since the amount of destabilized asphaltenes is relatively small, agglomerates can slowly grow as big as possible and precipitate separately (diffusion-limited aggregation)[76−78] forming sediment-like deposit. Slow aggregation of asphaltenes and their removal from the solution phase results in gradual change of the upper phase composition, which is observed by the T_2 relaxation time increase for the upper phase (Figure 12).

So, depending on the heptane volume ratio, we can observe two types of asphaltene precipitation: the formation of suspension with a power-law collapse of the sedimentation front (Case 1) and accumulation of sediment-like deposit with a rising front (Case 2). Moreover, ATR-FTIR spectroscopic imaging data suggest that the reason for these different behaviors of deposit is a result of the chemical composition of the asphaltene species. Oxygen- and nitrogen-abundant asphaltenes are less stable due to the ability for strong intermolecular interactions to be formed. Such asphaltenes can be easily destabilized by small concentrations of heptane forming separate agglomerates, which settle as sediment-like deposits. On the contrary, asphaltenes with high aromatic content are more soluble in the crude oil/heptane blend and are destabilized by a relatively high amount of heptane. Under such conditions, these type of asphaltenes give a colloidal suspension that consisted of agglomerates, which further turns to a gel-like deposit.

5. CONCLUSION

ATR-FTIR and NMR spectroscopic imaging approaches were used in this work to study crude oil samples under various conditions of dilution with heptane. Importantly, while ATR-FTIR spectroscopic imaging is particularly suited to study precipitation in such systems, NMR imaging can analyze the bulk phases. The precipitate formation and evolution were observed and monitored in the case of each sample at particular crude oil/heptane ratios. Based on the ATR-FTIR spectra, precipitates were identified as asphaltenes having various chemical constituents. Application of NMR imaging to study crude oil behavior in situ allowed three types of crude oil/heptane behaviors to be established that result in different phase equilibrium. The formation of the gel-like and sediment-like deposits was found for blends depending on the asphaltenes and flocculant concentrations. These deposit phases are different in terms of their structure and phase behavior. Using the data obtained by ATR-FTIR spectroscopic imaging and NMR imaging the chemical composition of asphaltenes was brought into correlation with their stability and behavior during precipitation.

Relatively small amounts of heptane cause the aggregation of the most unstable asphaltenes, which have a tendency for stronger intermolecular interactions due to the presence of oxygen- and nitrogen-containing functional groups. The number of such asphaltenes in crude oil is low, thus they give sediment-like deposit, which consists of particles settling separately. High concentrations of heptane result in major part of asphaltene fraction, consisting of aromatic species predominantly, aggregation followed by precipitation. The precipitation is occurring via hindered settling due to the relatively large amount of precipitated material giving gel-like deposit.

Thus, the benefits of the combined application of two complementary methods, namely ATR-FTIR spectroscopic imaging and NMR imaging, have been demonstrated. Providing in situ data on properties of asphaltenes and crude oils, these approaches are able to provide valuable insight into the mechanisms of deposit formation and to reveal correlations between molecular chemical composition and bulk phase behavior.

AUTHOR INFORMATION

Corresponding Authors

*O.N.M.: E-mail: oleg@catalysis.ru.

*S.G.K.: E-mail: s.kazarian@imperial.ac.uk.

Notes

The authors declare no competing financial interest.

ACKNOWLEDGMENTS

This research was performed under the UNIHEAT project. The authors wish to acknowledge the Skolkovo Foundation and BP for financial support. The authors thank BP for providing samples of crude oil.

REFERENCES

(1) Mullins, O. C.; Sheu, E. Y.; Hammami, A.; Marshall, A. G. *Asphaltenes, Heavy Oils, and Petroleomics*; Springer: New York, NY, 2007.

(2) Leontaritis, K. J.; Mansoori, G. A. Asphaltene Deposition: A Survey of Field Experiences and Research Approaches. *J. Pet. Sci. Eng.* **1988**, *1*, 229−239.

(3) Wiehe, I. A.; Liang, K. S. Asphaltenes, Resins, and Other Petroleum Macromolecules. *Fluid Phase Equilib.* **1996**, *117*, 201−210.

(4) Sirota, E. B. Physical Structure of Asphaltenes. *Energy Fuels* **2005**, *19*, 1290−1296.

(5) Groenzin, H.; Mullins, O. C. Molecular Size and Structure of Asphaltenes from Various Sources. *Energy Fuels* **2000**, *14*, 677−684.

DOI: 10.1021/jp511891f
J. Phys. Chem. C 2015, 119, 2646−2660

(6) Ting, P. D.; Hirasaki, G. J.; Chapman, W. G. Modeling of Asphaltene Phase Behavior with the SAFT Equation of State. *Pet. Sci. Technol.* **2003**, *21*, 647−661.
(7) Mannistu, K. D.; Yarranton, H. W.; Masliyah, J. H. Solubility Modeling of Asphaltenes in Organic Solvents. *Energy Fuels* **1997**, *11*, 615−622.
(8) Branco, V. A. M.; Mansoori, G. A.; De Almeida Xavier, L. C.; Park, S. J.; Manafi, H. Asphaltene Flocculation and Collapse from Petroleum Fluids. *J. Pet. Sci. Eng.* **2001**, *32*, 217−230.
(9) Victorov, A. I.; Firoozabadi, A. Thermodynamic Micellizatin Model of Asphaltene Precipitation from Petroleum Fluids. *AlChE J.* **1996**, *42*, 1753−1764.
(10) Wu, J.; Prausnitz, J. M.; Firoozabadi, A. Molecular-Thermodynamic Framework for Asphaltene-Oil Equilibria. *AlChE J.* **1998**, *44*, 1188−1199.
(11) Buenrostro-González, E.; Lira-Galeana, C.; Gil-Villegas, A.; Wu, J. Asphaltene Precipitation in Crude Oils: Theory and Experiments. *AIChE J.* **2004**, *50*, 2552−2570.
(12) Hirschberg, A.; de Jong, L. N. J.; Schipper, B. A.; Maijer, J. G. Influence of Temperature and Pressure on Asphaltene Flocculation. *Soc. Pet. Eng. J.* **1984**, *24*, 283−293.
(13) Sirota, E. B.; Lin, M. Y. Physical Behavior of Asphaltenes. *Energy Fuels* **2007**, *21*, 2809−2815.
(14) Andersen, S. I.; Birdi, K. S. Aggregation of Asphaltenes as Determined by Calorimetry. *J. Colloid Interface Sci.* **1991**, *142*, 497−502.
(15) Andersen, S. I.; Jensen, J. O.; Speight, J. G. X-ray Diffraction of Subfractions of Petroleum Asphaltenes. *Energy Fuels* **2005**, *19*, 2371−2377.
(16) Andreatta, G.; Bostrom, N.; Mullins, O. C. High-Q Ultrasonic Determination of the Critical Nanoaggregate Concentration of Asphaltenes and the Critical Micelle Concentration of Standard Surfactants. *Langmuir* **2005**, *21*, 2728−2736.
(17) Andrews, A. B.; Guerra, R. E.; Mullins, O. C.; Sen, P. N. Diffusivity of Asphaltene Molecules by Fluorescence Correlation Spectroscopy. *J. Phys. Chem. A* **2006**, *110*, 8093−8097.
(18) Auflem, I.; Havre, T.; Sjöblom, J. Near-IR study on the Dispersive Effects of Amphiphiles and Naphthenic Acids on Asphaltenes in Model Heptane-Toluene Mixtures. *Colloid Polym. Sci.* **2002**, *280*, 695−700.
(19) Bouhadda, Y.; Bormann, D.; Sheu, E.; Bendedouch, D.; Krallafa, A.; Daaou, M. Characterization of Algerian Hassi-Messaoud asphaltene structure using Raman spectrometry and X-ray diffraction. *Fuel* **2007**, *86*, 1855−1864.
(20) Burya, Y. G.; Yudin, I. K.; Dechabo, V. A.; Kosov, V. I.; Anisimov, M. A. Light-Scattering Study of Petroleum Asphaltene Aggregation. *Appl. Opt.* **2001**, *40*, 4028−4035.
(21) Eyssautier, J. l.; Levitz, P.; Espinat, D.; Jestin, J.; Gummel, J.; Grillo, I.; Barré, L. c. Insight into Asphaltene Nanoaggregate Structure Inferred by Small Angle Neutron and X-ray Scattering. *J. Phys. Chem. B* **2011**, *115*, 6827−6837.
(22) Lisitza, N. V.; Freed, D. E.; Sen, P. N.; Song, Y.-Q. Study of Asphaltene Nanoaggregation by Nuclear Magnetic Resonance (NMR). *Energy Fuels* **2009**, *23*, 1189−1193.
(23) Mostowfi, F.; Indo, K.; Mullins, O. C.; McFarlane, R. Asphaltene Nanoaggregates Studied by Centrifugation. *Energy Fuels* **2008**, *23*, 1194−1200.
(24) Rogel, E.; León, O.; Torres, G.; Espidel, J. Aggregation of Asphaltenes in Organic Solvents Using Surface Tension Measurements. *Fuel* **2000**, *79*, 1389−1394.
(25) Tagirzyanov, M. I.; Yakubov, M. R.; Romanov, G. V. A Study of the Processes Related to Coagulation of Asphaltenes by Electronic Spin Resonance. *J. Can. Pet. Technol.* **2007**, *46*, 9−13.
(26) Tuzikov, F. V.; Larichev, Y. V.; Borisova, L. S.; Kozhevnikov, I. V.; Mart'yanov, O. N. Small-Angle Scattering Study of Colloidal Particles in Heavy Crude Oils. *Pet. Chem.* **2011**, *51*, 281−285.
(27) Wattana, P.; Wojciechowski, D. J.; Bolaños, G.; Fogler, H. S. Study of Asphaltene Precipitation Using Refractive Index Measurement. *Pet. Sci. Technol.* **2003**, *21*, 591−613.
(28) Zajac, G. W.; Sethi, N. K.; Joseph, J. T. Molecular Imaging of Petroleum Asphaltenes by Scanning-Tunneling-Microscopy − Verification of Structure from C-13 and Proton Nuclear-Magnetic-Resonance Data. *Scanning Microsc.* **1994**, *8*, 463−470.
(29) Trukhan, S. N.; Yudanov, V. F.; Gabrienko, A. A.; Subramani, V.; Kazarian, S. G.; Martyanov, O. N. In-situ ESR Study of Molecular Dynamics of Asphaltenes at Elevated Temperature and Pressure. *Energy Fuels* **2014**, *28*, 6315−6321.
(30) Kokal, S. L.; Najman, J.; Sayegh, S. G.; George, A. E. Measurement and Correlation of Asphaltene Precipitation from Heavy Oils by Gas Injection. *J. Can. Pet. Technol.* **1992**, *31*, 24−30.
(31) Huang, J.; Yuro, R.; Romeo, G. A., Jr. Photooxidation of Corbett Fractions of Asphalt. *Fuel Sci. Technol. Int.* **1995**, *13*, 1121−1134.
(32) Castro, L. V.; Vazquez, F. Fractionation and Characterization of Mexican Crude Oils. *Energy Fuels* **2009**, *23*, 1603−1609.
(33) Cooper, J. B.; Wise, K. L.; Welch, W. T.; Sumner, M. B.; Wilt, B. K.; Bledsoe, R. R. Comparison of Near-IR, Raman, and Mid-IR Spectroscopies for the Determination of BTEX in Petroleum Fuels. *Appl. Spectrosc.* **1997**, *51*, 1613−1620.
(34) Coelho, R. R.; Hovell, I.; Moreno, E. L.; de Souza, A. L.; Rajagopal, K. Characterization of Functional Groups of Asphaltenes in Vacuum Residues Using Molecular Modelling and FTIR Techniques. *Pet. Sci. Technol.* **2007**, *25*, 41−54.
(35) Coelho, R. R.; Hovell, I.; Monte, M. B. M.; Middea, A.; de Souza, A. L. Characterisation of Aliphatic Chains in Vacuum Residues (VRs) of Asphaltenes and Resins Using Molecular Modelling and FTIR techniques. *Fuel Process. Technol.* **2006**, *87*, 325−333.
(36) Christy, A. A.; Dahl, B.; Kvalheim, O. M. Structural Features of Resins, Asphaltenes and Kerogen Studied by Diffuse Reflectance Infrared Spectroscopy. *Fuel* **1989**, *68*, 430−435.
(37) Buenrostro-González, E.; Espinosa-Peña, M.; Andersen, S. I.; Lira-Galeana, C. Characterization of Asphaltenes and Resins from Problematic Mexican Crude Oils. *Pet. Sci. Technol.* **2001**, *19*, 299−316.
(38) de Peinder, P.; Visser, T.; Petrauskas, D. D.; Salvatori, F.; Soulimani, F.; Weckhuysen, B. M. Partial Least Squares Modeling of Combined Infrared, ^{1}H NMR and ^{13}C NMR Spectra to Predict Long Residue Properties of Crude Oils. *Vib. Spectrosc.* **2009**, *51*, 205−212.
(39) Curtis, V.; Nicolaides, C. P.; Coville, N. J.; Hildebrandt, D.; Glasser, D. The Effect of Sulfur on Supported Cobalt Fischer−Tropsch Catalysts. *Catal. Today* **1999**, *49*, 33−40.
(40) Parisotto, G.; Ferrão, M. F.; Müller, A. L. H.; Müller, E. I.; Santos, M. F. P.; Guimarães, R. C. L.; Dias, J. C. M.; Flores, E. M. M. Total Acid Number Determination in Residues of Crude Oil Distillation Using ATR-FTIR and Variable Selection by Chemometric Methods. *Energy Fuels* **2010**, *24*, 5474−5478.
(41) Orrego-Ruiz, J. A.; Guzmán, A.; Molina, D.; Mejía-Ospino, E. Mid-Infrared Attenuated Total Reflectance (MIR-ATR) Predictive Models for Asphaltene Contents in Vacuum Residua: Asphaltene StructureFunctionality Correlations Based on Partial Least-Squares Regression (PLS-R). *Energy Fuels* **2011**, *25*, 3678−3686.
(42) Coelho, R. R.; Hovell, I.; Rajagopal, K. Elucidation of the Functional Sulphur Chemical Structure in Asphaltenes Using First Principles and Deconvolution of Mid-Infrared Vibrational Spectra. *Fuel Process. Technol.* **2012**, *97*, 85−92.
(43) Müller, A. L. H.; Picoloto, R. S.; Mello, P. A.; Ferrão, M. F.; dos Santos, M. F. P.; Guimarães, R. C. L.; Müllera, E. I.; Flores, E. M. M. Total Sulfur Determination in Residues of Crude Oil Distillation Using FT-IR/ATR and Variable Selection Methods. *Spectrochim. Acta* **2012**, *89*, 82−87.
(44) Tay, F. H.; Kazarian, S. G. Study of Petroleum Heat-exchanger Deposits with ATR-FTIR Spectroscopic Imaging. *Energy Fuels* **2009**, *23*, 4059−4067.
(45) Gabrienko, A. A.; Lai, C. H.; Kazarian, S. G. In Situ Chemical Imaging of Asphaltene Precipitation from Crude Oil Induced by n-Heptane. *Energy Fuels* **2014**, *28*, 964−971.
(46) Gabrienko, A. A.; Subramani, V.; Martyanov, O. N.; Kazarian, S. G. Correlation between Asphaltene Stability in n-Heptane and Crude Oil Composition Revealed with In Situ Chemical Imaging. *Adsorpt. Sci. Technol.* **2014**, *32*, 243−255.

DOI: 10.1021/jp511891f
J. Phys. Chem. C 2015, 119, 2646−2660

(47) Acosta-Cabronero, J.; Hall, L. D. Measurements by MRI of the Settling and Packing of Solid Particles from Aqueous Suspensions. *AlChE J.* **2009**, *55*, 1426−1433.
(48) Beyea, S. D.; Altobelli, S. A.; Mondy, L. A. Chemically Selective NMR Imaging of a 3-Component (Solid−Solid−Liquid) Sedimenting System. *JMagR* **2003**, *161*, 198−203.
(49) Koptyug, I. V.; Lysova, A. A.; Kovtunov, K. V.; Zhivonitko, V. V.; Khomichev, A. V.; Sagdeev, R. Z. Multinuclear Magnetic Resonance Imaging as a Multifunctional Tool for the Investigation of the Properties of Materials, Transport Processes and Catalytic Reactions. *Russ. Chem. Rev.* **2007**, *76*, 583−598.
(50) Miknis, F. P.; Pauli, A. T.; Beemer, A.; Wilde, B. Use of NMR Imaging to Measure Interfacial Properties of Asphalts. *Fuel* **2005**, *84*, 1041−1051.
(51) Miknis, F. P.; Pauli, A. T.; Michon, L. C.; Netzel, D. A. NMR Imaging Studies of Asphaltene Precipitation in Asphalts. *Fuel* **1998**, *77*, 399−405.
(52) Morozov, E. V.; Martyanov, O. N.; Volkov, N. V.; Falaleev, O. V. NMR Imaging of Heavy Crude Oil for Softening Detection under Heat Treatment. *J. Mater. Sci. Eng.: A* **2011**, *1*, 545−551.
(53) Stapf, S.; Han, S.-I. *NMR Imaging in Chemical Engineering*; WILEY-VCH: Weinheim, Germany, 2006.
(54) Gladden, L. F.; Mantle, M. D.; Sederman, A. J. Magnetic Resonance Imaging of Catalysts and Catalytic Processes. In *Advances in Catalysis*; Gates, B. C., Knozinger, H., Eds.; Elsevier Academic Press Inc: San Diego, CA, 2006; Vol *50*.
(55) Mitchell, J.; Chandrasekera, T. C.; Holland, D. J.; Gladden, L. F.; Fordham, E. J. Magnetic Resonance Imaging in Laboratory Petrophysical Core Analysis. *Phys. Rep.* **2013**, *526*, 165−225.
(56) Chan, K. L. A.; Kazarian, S. G. Detection of Trace Materials with Fourier Transform Infrared Spectroscopy Using a Multi-Channel Detector. *Analyst* **2006**, *131*, 126−131.
(57) Ricci, C.; Phiriyavityopas, P.; Curum, N.; Chan, K. L. A.; Jickells, S.; Kazarian, S. G. Chemical Imaging of Latent Fingerprint Residues. *Appl. Spectrosc.* **2007**, *61*, 514−522.
(58) Kazarian, S. G.; Chan, K. L. A. Micro- and Macro-Attenuated Total Reflection Fourier Transform Infrared Spectroscopic Imaging. *Appl. Spectrosc.* **2010**, *64*, 135A−152A.
(59) Callaghan, P. *Principles of Nuclear Magnetic Resonance Microscopic*; Clarendon Press: Oxford, UK, 1993.
(60) Bernstein, M. A.; King, K. F.; Zhou, X. J. *Handbook of MRI Pulse Sequences*; Elsevier Academic Press: Burlington, MA, 2004.
(61) Colangeli, L.; Mennella, V.; Baratta, G. A.; Bussoletti, E.; Strazzulla, G. Raman and Infrared Spectra of Polycyclic Aromatic Hydrocarbon Molecules of Possible Astrophysical Interest. *Astrophys. J.* **1992**, *396*, 369−377.
(62) Staggs, R. L.; Lyon, W. G. FT-IR Solution Spectra of Propyl Sulfide, Propyl Sulfoxide, and Propyl Sulfone. *Appl. Spectrosc.* **1995**, *49*, 1772−1775.
(63) Klots, T. D.; Chirico, R. D.; Steele, W. V. Complete Vapor Phase Assignment for the Fundamental Vibrations of Furan, Pyrrole and Thiophene. *Spectrochim. Acta* **1994**, *50*, 765−795.
(64) Angle, C. W.; Long, Y.; Hamza, H.; Lue, L. Precipitation of Asphaltenes from Solvent-Diluted Heavy oil and Thermodynamic Properties of Solvent-Diluted Heavy Oil Solutions. *Fuel* **2006**, *85*, 492−506.
(65) Maqbool, T.; Balgoa, A. T.; Fogler, H. S. Revisiting Asphaltene Precipitation from Crude Oils: A Case of Neglected Kinetic Effects. *Energy Fuels* **2009**, *23*, 3681−3686.
(66) Hoepfner, M. P.; Vilas Bôas FáVero, C.; Haji-Akbari, N.; Fogler, H. S. The Fractal Aggregation of Asphaltenes. *Langmuir* **2013**, *29*, 8799−8808.
(67) Mullins, O. C. The Asphaltenes. *Annu. Rev. Anal. Chem.* **2011**, *4*, 393−418.
(68) Mullins, O. C.; Sabbah, H.; Eyssautier, J.; Pomerantz, A. E.; Barré, L.; Andrews, A. B.; Ruiz-Morales, Y.; Mostowfi, F.; McFarlane, R.; Goual, L.; Lepkowicz, R.; Cooper, T.; Orbulescu, J.; Leblanc, R. M.; Edwards, J.; Zare, R. N. Advances in Asphaltene Science and the Yen−Mullins Model. *Energy Fuels* **2012**, *26*, 3986−4003.
(69) Sedghi, M.; Goual, L.; Welch, W.; Kubelka, J. Effect of Asphaltene Structure on Association and Aggregation Using Molecular Dynamics. *J. Phys. Chem. B* **2013**, *117*, 5765−5776.
(70) Mutelet, F.; Ekulu, G.; Solimando, R.; Rogalski, M. Solubility Parameters of Crude Oils and Asphaltenes. *Energy Fuels* **2004**, *18*, 667−673.
(71) Murgich, J.; Abanero, J. A.; Strausz, O. P. Molecular Recognition in Aggregates Formed by Asphaltene and Resin Molecules from the Athabasca Oil Sand. *Energy Fuels* **1999**, *13*, 278−286.
(72) Morozov, E. V.; Shabanova, O. V.; Falaleev, O. V. MRI Comparative Study of Container Geometry Impact on the PMMA Spheres Sedimentation. *Appl. Magn. Reson.* **2013**, *44*, 619−636.
(73) Kynch, G. J. A Theory of Sedimentation. *Trans. Faraday Soc.* **1952**, *48*, 166−176.
(74) Altobelli, S. A.; Mondy, L. A. Hindered Flotation Functions from Nuclear Magnetic Resonance Imaging. *J. Rheol. (Melville, NY, U.S.)* **2002**, *46*, 1341−1352.
(75) Turney, M. A.; Cheung, M. K.; Powell, R. L.; McCarthy, M. J. Hindered Settling of Rod-Like Particles Measured with Magnetic Resonance Imaging. *AlChE J.* **1995**, *41*, 251−257.
(76) Hashmi, S. M.; Firoozabadi, A. Effect of Dispersant on Asphaltene Suspension Dynamics: Aggregation and Sedimentation. *J. Phys. Chem. B* **2010**, *114*, 15780−15788.
(77) Hashmi, S. M.; Quintiliano, L. A.; Firoozabadi, A. Polymeric Dispersants Delay Sedimentation in Colloidal Asphaltene Suspensions. *Langmuir* **2010**, *26*, 8021−8029.
(78) Poon, W. C. K.; Starrs, L.; Meeker, S. P.; Moussaid, A.; Evans, R. M. L.; Pusey, P. N.; Robins, M. M. Delayed Sedimentation of Transient Gels in Colloid-Polymer Mixtures: Dark-Field Observation, Rheology and Dynamic Light Scattering Studies. *Faraday Discuss.* **1999**, *112*, 143−154.

DOI: 10.1021/jp511891f
J. Phys. Chem. C 2015, 119, 2646−2660